E3S Web of Conferences **271**, 03003 (2021) https://doi.org/10.1051/e3sconf/202127103003
ICEPE 2021

Research on the Influencing Factors of Air-puff Test after SMILE Based on Finite Element Analysis

Luchao Lin[1], Lihua Fang[1,*], Xingming Tao[1], Yinyu Song[1], Ruirui Du[1]

[1]Key Laboratory of Nondestructive Test (Ministry of Education), Nanchang Hangkong University, Nanchang, 330063, China

Abstract: The three-dimensional finite element model of the postoperative whole human eye after small incision lenticule extraction (SMILE) surgery and the axisymmetric air-puff model were established, the influencing factors in the Air-puff test were explored from the displacement nephogram on anterior corneal surface. Our results showed that the maximum depression displacement was positively correlated with the corrected diopter when the peak pressure of ejection and air-puff center location were constant, but the highest concavity radius of concave curvature was negatively correlated with the corrected diopter. At the same time, we also found that when the decentration of air-puff center position was 1mm, the maximum depression displacement of the anterior corneal surface was reduced by 8.3% under the condition of constant correction diopter and peak air-puff pressure, compared with the maximum depression displacement of the anterior corneal surface when the decentration of air-puff center position was 0 mm. In conclusion, the corrected diopter and decentration of air-puff position have an important effect on the results of air-puff test after SMILE.

1 Introduction

With flapless and small incision, SMILE has high safety, effectiveness, predictability and stability in correcting visual acuity. However, the refractive surgery makes the cornea thinner and leads to changes in biomechanical properties, postoperative patients are at risk of refractive instability and corneal dilatation[1]. Therefore, it is of great significance to study the biomechanical properties of human eyes after SMILE, and it can also provide theoretical basis for clinical practice[2]. IB Pedersen et al.[3] used Corvis-ST comparison to analyze the biomechanical changes of 29 eyes after Smile and 31 healthy eyes.

Air-puff method is a non-contact dynamic measurement method, which can avoid secondary damage to eyes and is widely used in clinic[4]. At present, ocular response analyzer (ORA) and Corneal Visualization Scheimpflug technology (Corvis-ST) are commonly used in clinic, both of which use air-puff method to deform the cornea[5, 6]. In addition, there have been some studies on simulated corneal dynamic parameters. MontaninA et al[7]. studied a numerical model of non-contact measurement to explore the biomechanical properties of human cornea through fluid-solid coupling, but his model only used cornea and did not take into account the effects of other structures and tissues.

In this paper, based on the 3D solid model and axisymmetric air-puff model of human eye, the finite element analysis software ANSYS was used to explore the biomechanical effects of corrected diopter, air-puff pressure and air-puff eccentricity on the eyes after SMILE.

2 Materials and Methods

2.1 Material properties

L-YWOO et al.[8] shown that the material properties of cornea and sclera were nonlinear which could be represented using the super elastic material model of the ogden strain energy function[9,10]. Its strain energy functions are as follows:

$$W = \sum_{i=1}^{N} \frac{\mu_i}{\alpha_i}(\overline{\lambda_1}^{\alpha_i} + \overline{\lambda_2}^{\alpha_i} + \overline{\lambda_3}^{\alpha_i} - 3) + \sum_{k=1}^{N} \frac{1}{d_i}(j-1)^{2k} \quad (1)$$

W represents the strain energy. λ_1, λ_2, λ_3 represent elongation at each main direction. J represents the row of deformation gradient matrices. N, μ_i, α_i and d_i represent various material parameters, super elasticity and compression of materials.

Considering the irrecomability of the corneal tissue material, its strain energy function can be expressed as:

$$W = \sum_{i=1}^{N} \frac{\mu_i}{\alpha_i}(\overline{\lambda_1}^{\alpha_i} + \overline{\lambda_2}^{\alpha_i} + \overline{\lambda_3}^{\alpha_i} - 3) \quad (2)$$

With the fitting analysis of experimental data, the fitting parameters of cornea are μ_1=0.035357MPa, α_1=103.61; μ_2=0.026728MPa, α_2=100.58.

* Corresponding author: fanglh71@126.com

2.2 Three-Dimensional eye model and air puff model

Since the jet process in the experiment is faster, only the flexible characteristics of the cornea and the sclera is considered to ignore the viscoelastic characteristics[11]. Select a shaft symmetrical dynamic air-puff model[10].

Air-puff pressure can be expressed as follows:

$$P_{\text{jet}}(X,t) = P_{peak}\exp(-dr^2)\exp[-b(\frac{t}{T}-\frac{1}{2})^2], r^2 < R^2 \quad (3)$$

R is a radius (mm) of the front surface jet range of the cornea. R is the distance (mm) between the front surface and the air puff center of the cornea. P_{Peak} is a peak pressure (KPa). T is the total air-puff time (ms). b, d is the pressure distribution parameter of the control time. Here, R=1.5mm, T=30ms, d=0.44, b=25.

The grid division adopts the hexahedral dominating method, of which the number of nodes of the cornea is 74385, the number of mesh cells is 18891; the number of nodes of the scleral is 65352, the number of mesh cells is 18704. The fixation constraint was set at the posterior pole of scleral model. The air-puff results were shown below:

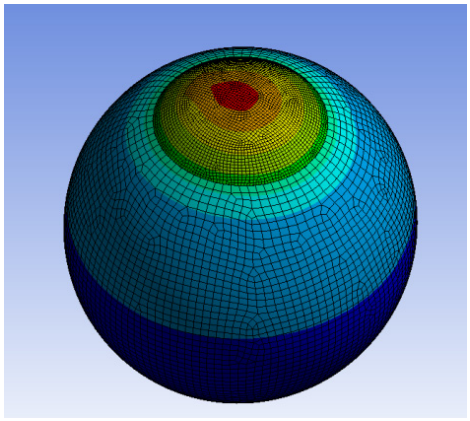

Fig. 1. Post -6D results after application of air-puff pressure

2.3 SMILE surgery simulation

The refractiveness before the initial surgery is S, the unit is D, and the postoperative is 0D and their mathematical expression is as follows:

$$S = (\mathrm{n}-1)(\frac{1}{L}-\frac{1}{R_1}) \quad (4)$$

R1 represents the curvature radius of the anterior surface of the preoperative cornea, L is the curvature radius of the anterior surface of the postoperative cornea, and N is the refractive index of the cornea, which is 1.376.

According to the geometric relationship of the postoperative and postoperative corneal surface, the depth of corneal lenticule was calculated.

$$I(r) = \sqrt{R_1^2 - r^2} - \sqrt{[\frac{(n-1)R_1}{n-1+SR_1}]^2 - r^2} + \sqrt{[\frac{(n-1)R_1}{n-1+SR_1}]^2 - (O/2)^2} - \sqrt{R_1^2 - (O/2)^2} \quad (5)$$

O is the diameter of the optical zone.

According to the cutting principle of SMILE surgery, a 3D finite element model of the postoperative eye was constructed to simulate SMILE refractive surgery[12].

3 Results

3.1 Effect of corrective diopter on the test

A numerical air-puff model was constructed and the material parameters of cornea and sclera were set. The intraocular pressure was 18mmHg, the peak air injection pressure was 40kPa, and the corrected diopter was -1D to -10D. According to the nephogram of the anterior corneal surface displacement results, the corneal morphological parameters after SMILE under different corrected diopter were obtained by using the curved surface fitting method. The results were shown below:

Table 1. The corneal morphology parameters under different diopters when the intraocular pressure was 18mmHg and the ejection pressure was 40KPa

Diopter（D）	Maximum depression time(ms)	Maximum apical corneal displacement(mm)	Highest Concavity Radius of Concave Curvature(mm)
-1D	15.5	1.8557	3.257
-2D	15.5	1.9084	3.0517
-3D	15.5	1.9572	2.8588
-4D	15	2.005	2.7446
-5D	15	2.0435	2.6451
-6D	15	2.0767	2.5382
-7D	15	2.1054	2.4495
-8D	15	2.1304	2.4057
-9D	15	2.1528	2.3269
-10D	15	2.1752	2.2949

From Table 1, the analysis of air-puff test after each diopter shows that the maximum corneal deformation occurs near 15ms. With the increased of corrected diopter, the maximum depression displacement at the top of the anterior corneal surface increased gradually, and the maximum apical corneal displacement of the corrected diopter -10D was 17.2% larger than that of the corrected diopter -1D. And the highest concavity radius of concave curvature of the anterior corneal surface decreases with the increased of corrected diopter. When the corrected diopter was -10D, the highest concavity radius of concave curvature decreased by 25.9% compared with

that of -1D. The results showed that refractive surgery has a significant effect on the biomechanical properties of cornea after operation. There were significant changes in corneal morphological parameters after air-puff test after operation.

3.2 Effect of air-puff eccentricity on test

Based on the 3D finite element whole eye model after SMILE with corrective diopter of -6D, the axisymmetric air-puff model was used to set the peak jet pressure to 40KPa. The lateral offset of the air-puff center was set to 0.2mm, 0.4mm, 0.6mm, 0.8mm and 1mm, respectively.

Table 2. Corneal morphological parameters under lateral offset of different jet centers when corrected diopter -6D and peak jet pressure 40KPa

Lateral offset of air-puff center（mm）	Maximum apical corneal displacement（mm）	Highest Concavity Radius of Concave Curvature（mm）	Maximum depression position offset（mm）
0.2	2.067	2.4222	0.0959
0.4	2.03333	2.4488	0.1921
0.6	1.9842	2.4931	0.2839
0.8	1.9128	2.6008	0.3662
1	1.9032	2.6154	0.49514

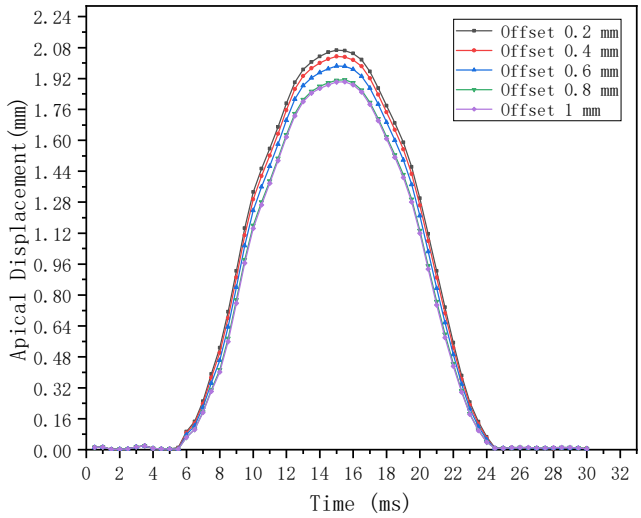

Fig.2. Corneal apical displacement with time variation curve during transverse offset different air-puff center

According to figure 2, under different lateral offset of the air-puff center, the corneal apical displacement increased at first and then decreased during the air-puff process. And the largest depression appeared in 15ms in all tests. From table 2, the maximum depression displacement at the top of the cornea was negatively correlated with the lateral offset of the air-puff center. The maximum apical displacement of the air-puff center lateral offset 1mm is 8.3% less than that of the offset 0mm. However, there was a positive correlation between the highest concavity radius of concave curvature and the lateral offset of the air-puff center. The highest concavity radius of concave curvature increased by 3% when the air-puff center lateral offset 1mm compared with the offset 0mm. The maximum depression position offset increased with the increased of the lateral offset of the air-puff center.

4 Conclusion

In this paper, based on the 3D finite element whole eye model and air-puff model after SMILE, the influencing factors of air-puff experiment after SMILE were analyzed theoretically. The results showed that corrective diopter and air-puff eccentricity have important influence on the results of air-puff test after SMILE.

Acknowledgments

Supported by Natural National Science Foundation of China(NSFC)(61465010), National Key Research and Development Program of China (2018YFE0115700) and Jiangxi Nature Science Foundation (20192BAB207035). Have no conflicts of interest.

Reference

1. M. Liu, Y. Chen, D. Wang, Y. Zhou, and L. Quan, "Clinical Outcomes After SMILE and Femtosecond Laser-Assisted LASIK for Myopia and Myopic Astigmatism: A Prospective Randomized Comparative Study," *Cornea,* vol. **35**(2): P. 210 (2015).
2. F. Mathew *et al.*, "In Vivo Prediction of Air-Puff Induced Corneal Deformation Using LASIK, SMILE, and PRK Finite Element Simulations," *Invest Ophth Vis Sci,* vol. **59**(13): P. 5320-5328 (2018).
3. I. B. Pedersen, S. Bak-Nielsen, A. H. Vestergaard, A. Ivarsen, and J. Hjortdal, "Corneal biomechanical properties after LASIK, ReLEx flex, and ReLEx smile by Scheimpflug-based dynamic tonometry," *Graef Arch Clin Exp,* vol. **252**(8): P. 1329-1335 (2014).
4. I. Simonini and A. Pandolfi, "The influence of intraocular pressure and air jet pressure on corneal contactless tonometry tests," *J Mech Behav Biomed Mater,* vol. **58**(1):P. 75-89 (2016).
5. M. Sullivan-Mee, G. Gerhardt, K. D. Halverson, and C. Qualls, "Repeatability and reproducibility for intraocular pressure measurement by dynamic contour, ocular response analyzer, and goldmann applanation tonometry," *J Glaucoma,* vol. **18**(9): P. 666-73 (2009).
6. L. Ramm, R. Herber, E. Spoerl, F. Raiskup, and N. Terai, "Intraocular Pressure Measurement Using Ocular Response Analyzer, Dynamic Contour Tonometer, and Scheimpflug Analyzer Corvis ST," *J Ophth,* vol. **2019**(6): P. 1-9 (2019).
7. A. Am, B. Ma, and A. Ap, "A 3D fluid-solid interaction model of the air puff test in the human cornea," *J Mech Behav Biomed,* vol. **94**(1): P. 22-31 (2019).
8. L. Y. Woo, A. S. Kobayashi, W. A. Schlegel, and C. Lawrence, "Nonlinear material properties of intact cornea and sclera," *Exp Eye Res,* vol. **14**(1): P. 29-39 (1972).
9. J. G. Yu, F. J. Bao, Y. F. Feng, C. Whitford, and A. Elsheikh, "Assessment of corneal biomechanical behavior under posterior and anterior pressure," *J Refract Surg,* vol. **29**(1): P. 64-70 (2013).
10. A. Montanino, M. Angelillo, and A. Pandolfi, "Modelling with a meshfree approach the cornea-aqueous humor interaction during the air puff test," (in eng), *J mech behav of biomed,* vol. **77**(1): P. 205-216 (2018).
11. Z. Han *et al.*, "Air Puff Induced Corneal Vibrations: Theoretical Simulations and Clinical Observations," *J Refract Surg,* vol. **30**(3): P. 208 (2014).
12. B. Vojnikovi and E. Tamajo, "Gullstrand's optical schematic system of the eye--modified by Vojnikovi & Tamajo," *Coll Antropol,* vol. **37** (Suppl 1): P. 41-45 (2013).